

## Application of Disposable Pipette Extraction for Determination of Yb by High-Resolution Continuum Source Graphite Furnace Atomic Absorption Spectrometry Using Lanthanum as a Chemical Modifier

Diogo M. Betiolo,<sup>a</sup> Heloisa R. Cadorim,<sup>a</sup> Eduardo Carasek<sup>✉</sup>\*<sup>a</sup> and Tatiane A. Maranhão<sup>✉</sup><sup>a</sup>

<sup>a</sup>Departamento de Química, Universidade Federal de Santa Catarina, 88040-900 Florianópolis-SC, Brazil

The use of extraction technique with disposable tips (DPX) was applied for the first time for the extraction and preconcentration of Yb in samples of liquid waste from the petrochemical industry and environmental water using bioabsorbent cork. The use of cork as an extracting phase in the determination of Yb by high-resolution continuum source graphite furnace atomic absorption spectrometry (HR-CS GF AAS) was evaluated. The pyrolysis and atomization temperatures were optimized at 1400 and 2400 °C, respectively. H<sub>2</sub>SO<sub>4</sub>, HNO<sub>3</sub> and HCl acids were compared in the steps of cleaning the extraction phase and desorption of the analyte by DPX. The best extraction in the selected conditions was obtained with pH 8.0 and 5% v/v HCl. The recoveries were close to 100% for residual water and drinking water, 33 to 77% for produced water and 64 to 93% for river water. Tests with interfering ions in different concentrations were performed. The relative limit of quantification (LOQ) and limit of detection (LOD) were estimated at 0.03 and 0.01 µg L<sup>-1</sup>, respectively. The total time for the preparation of the samples by DPX was close to 1 min *per* sample. Extraction and pre-concentration were observed using DPX with a pre-enrichment factor of approximately 4 times.

**Keywords:** ytterbium, residual water, environmental samples, sample preparation, DPX HR-CS GF AAS

### Introduction

The 17 elements of the REE (rare earth elements) group are considered metals with great applicability in modern technologies, as they present physical and chemical characteristics that distinguish them from other metals commonly used by industry.<sup>1</sup> In the last two decades, the use of REE has grown considerably, mainly in high-tech components such as electronics, but also in other areas such as military devices, medicine, agriculture and renewable energy.<sup>2-4</sup>

Ytterbium (Yb) is one of the most important elements of the REE group due to its unique properties and wide industrial application.<sup>5</sup> Its use is mainly in the manufacture of optical fibers, lasers, gas and vapor detection sensors, catalysts, luminescent materials, and nuclear fuel coating, among others.<sup>6-13</sup>

The increase in global demand and in the exploration of new sources of REE causes extra concern due to anthropic

actions, such as distribution and formation of new tailings containing these elements, which can be harmful to human health and the environment, even in low concentrations.<sup>14</sup> Ytterbium and its compounds can be harmful to human health, as they cause skin and eye irritation, may damage the structure of embryos or fetuses during pregnancy, and also present teratogenic potential.<sup>15,16</sup>

The generation of large amounts of waste by industries, such as petrochemical plants, accounts for a portion of the damage caused to the environment in general.<sup>1-4</sup> Thus, the quantification of the Yb fraction present in residual aqueous samples with high complexity becomes necessary.

The analytical techniques used to determine Yb are atomic absorption spectrometry with atomization in a graphite furnace (GF AAS), flame atomic absorption spectrometry (F AAS), inductively coupled plasma mass spectrometry (ICP-MS) and inductively coupled plasma optical emission spectrometry (ICP-OES). To a lesser extent, the techniques of X-ray fluorescence (XRF) and high-performance liquid chromatography with ultraviolet/visible detection are used (HPLC-UV/Vis), as described in specialized literature.<sup>17-19</sup>

\*e-mail: eduardo.carasek@ufsc.br

Editor handled this article: Emanuel Carrilho (Associate)

Despite the high sensitivity and agility obtained in techniques such as ICP-OES and ICP-MS, these require sample preparation to introduce the solution into the equipment. Consequently, the costs related to the preparation of samples with equipment dedicated to this function, as well as the necessary maintenance of ICP equipment, reduce its use in routine laboratory analyses. However, in some cases, preconcentration of the analyte and elimination of matrix interference may be necessary.<sup>17-20</sup>

The determination of metals at levels of  $\mu\text{g L}^{-1}$  to  $\text{ng L}^{-1}$  from direct analysis by atomization in a graphite furnace (GF AAS) is an effective way to reduce the sample preparation required by more sophisticated equipment, such as ICPs, and also possible interferences of the matrix. However, some interferences may manifest themselves during the analysis, mainly the formation of refractory carbides and oxides, memory effect and reduced graphite tube life.<sup>21,22</sup>

Alternative sample preparation techniques have been proposed in the literature, such as solid-phase microextraction (SPME),<sup>23</sup> dispersive liquid-liquid microextraction (DLLME),<sup>24</sup> dispersive solid-phase microextraction (DMSPE),<sup>25</sup> single drop microextraction (SDME)<sup>26</sup> and disposable pipette extraction (DPX),<sup>27,28</sup> these being used for the determination of metals at levels of  $\mu\text{g L}^{-1}$  to  $\text{ng L}^{-1}$ . DPX is a technique that has only recently been applied to sample preparation for the purpose of metal determination.

DPX was initially developed for the purpose of application in organic compounds. The technique consists of retaining an appropriate sorbent (extraction phase) between two filters inside the tip of a standard pipette. The aspiration of the liquid sample and air promotes a dynamic mixture, which leads to a rapid sorption equilibrium between the analyte and the extraction phase.<sup>29</sup> Consequently, it saves extraction time, providing satisfactory results for a series of analytes in different matrices.<sup>30</sup> The simplicity of the DPX mechanism brings other additional benefits, such as the removal of particulate materials that are retained in the filter and the sample matrix, which are released after the adsorption of the analyte in the extraction phase and ejection of the matrix from inside the pipette tip.

There are still few studies found in the literature regarding DPX for the determination of metals and, in particular, none reporting the determination of Yb with this technique so far.<sup>27,28</sup>

In this work, we present the application and optimization of DPX in the determination of Yb in environmental samples of residual water, produced water, river water and drinking water, by high-resolution continuum source graphite furnace atomic absorption spectrometry (HR-CS GF AAS). The application of DPX allowed

significant time savings, increased analytical frequency and reduced sample preparation steps. For the study, the optimization of the analyte atomization and the use of Doehlert and Box Behnken experimental designs were carried out in the optimization of the extraction and pre-concentration method by DPX.

## Experimental

### Instrumental and operational conditions

The measurements in the experiments were carried out using a high-resolution continuous source atomic absorption spectrometer (model ContrAA 700, Analytik Jena AG, Jena, Germany). For measurements, the Yb main line at 398.799 nm was used as the central pixel, using the sum of the integrated absorbance of three pixels (selected absorbance of peak volume, PVSA,  $A_{\Sigma 3, \text{int}}$ )<sup>31</sup> The measured spectral range comprises a range of 0.497 nm (398.554 to 399.051), equivalent to 200 pixels observable for analytical purposes. The operational parameters are described in Table 1.

**Table 1.** Operational parameters used for determination of Yb by HR-CS GF AAS

Parameter	
Wavelength / nm	398.799
Background correction mode	IBC
Scanned spectral range (wavelength) / nm	398.554-399.051
Scanned spectral range / pixel	200
Evaluation pixels	3
Read time / s	5
Integration mode	area
Sample volume / $\mu\text{L}$	20

IBC: iterative background correction.

The measurements were made using graphite tubes with pyrolytic coating with transverse heating and without a PIN platform (Analytik Jena, part number 407-A81.011). An AMPE60 automatic sampler (Analytik Jena) was used for the optimization of chemical modifiers and pyrolysis and atomization curves. The aqueous samples and standards were manually injected into the graphite tube with the aid of a micropipette. For analysis, a volume of 20  $\mu\text{L}$  of sample was injected manually into the graphite tube. The drying, pyrolysis, atomization and cleaning steps are shown in Table 2. Argonium (99.996%, White Martins, São Paulo, Brazil) was used as a purge and protection gas.

Disposable pipette tips used in the study as an extraction and pre-concentration device are commercially available

**Table 2.** Heating program used to optimize the pyrolysis and atomization curves in the determination of Yb in petrochemical industry waste by HR-CS GF AAS based on Aghabalazadeh *et al.*<sup>22</sup>

Step	Temperature / °C	Ramp / (°C s <sup>-1</sup> )	Hold / s	Purge
Drying	90	6	20	max
Drying	110	5	10	max
Pyrolysis	1400	300	10	max
Gas adaptation	1400	0	5	stop
Atomization	2400	FP	5	stop
Cleaning	2500	500	4	max

FP: full power; max: maximum.

(DPX Technologies, Columbia, SC, USA). The pipette tips used do not contain an extraction phase, only two filters at the ends to retain the material used as a sorbent. This type of tip allows the introduction of different sorbent materials as an extraction phase. A micropipette (HTL, Warsaw, Poland) with variable volume (100-1000 µL) was used in the experiments with DPX. For the comparison determination of Yb by ICP-MS, model ELAN 6000 equipment was used (PerkinElmer SCIEX, Shelton, USA).

The temperature program used for the thermal deposition of the modifiers inside the graphite tube is suggested by the manufacturer in the equipment's software. Aliquots of the modifying solution (La 1 g L<sup>-1</sup>, W 1 g L<sup>-1</sup> or Zr 1 g L<sup>-1</sup>) were injected with the aid of an automatic liquid sampler during 20 injection cycles of 50 µL. At the end of each injection, pre-drying is carried out at temperatures/times of 90 °C for 40 s, 110 °C for 40 s, 130 °C for 40 s. Finally, the 20 injections are subjected to a temperature of 1200 °C for 26 s and 2100 °C for 13 s.

## Reagents, solutions and samples

### Reagents and solutions

All reagents used in this study were analytical grade. Ultrapure water, with resistivity of 18.3 MΩ cm, was used for the preparation of standard solutions and for the cleaning of the extraction devices. It was obtained from model purification system Mega ROUP (Equisul, Pelotas, Brazil). Hydrochloric acid (Sigma-Aldrich, St. Louis, USA), sulfuric acid and nitric acid (Synth, São Paulo, Brazil) were used to prepare all standard solutions, cleaning and desorption of the analyte.

Solutions of NaOH (Vetec, Duque de Caxias, Brazil), anhydrous citric acid (Merck, New Jersey, USA), Na<sub>2</sub>HPO<sub>4</sub>, NaH<sub>2</sub>PO<sub>4</sub>, KH<sub>2</sub>PO<sub>4</sub> (Sigma-Aldrich) were used to prepare the buffer solution. Solutions of 1 g L<sup>-1</sup> of Zr (Fluka, St. Louis, USA), 1 g L<sup>-1</sup> of W (Sigma-Aldrich)

and 1 g L<sup>-1</sup> of La (Neon, Suzano, Brazil) were used as permanent chemical modifiers. Solution of 1 g L<sup>-1</sup> of Yb (Sigma-Aldrich) was used to prepare all standard solution and calibration curves in the experiments.

For the evaluation of sorbents, microcrystalline cellulose (Synth), phosphate cellulose (reproduced as in Kim *et al.*),<sup>32</sup> chitosan (Sigma-Aldrich), and locally acquired cork and bract were used.

The certified reference materials (CRMs) were digested in polytetrafluoroethylene (PTFE) vials with the aid of 5 mL of HNO<sub>3</sub> and 1 mL of HCl. The procedure was performed in an Ethos Plus microwave oven (Milestone, Sorisole, Italy). After digestion, they were made up to 25 mL with ultrapure water.

The following interferences in the form of cations and anions were evaluated: NaCl, KCl, Na<sub>2</sub>SO<sub>4</sub> and CH<sub>3</sub>COONa (Synth), NaNO<sub>3</sub> and Na<sub>2</sub>C<sub>2</sub>O<sub>4</sub> (Neon), Mg(NO<sub>3</sub>)<sub>2</sub> (Vetec), Ca(NO<sub>3</sub>)<sub>2</sub>, Al(NO<sub>3</sub>)<sub>3</sub> (Sigma-Aldrich). Initially, 500 mg L<sup>-1</sup> solutions were prepared for each interferent, and then dilutions were made according to the concentration to be studied (100, 1000, 2000, 3000 and 4000 times the analyte concentration).

### Samples and CRMs

Samples of petrochemical industry waste (produced water and sludge) were supplied by Petrobras (Brazil); river water and drinking water were acquired locally (Florianópolis, SC, Brazil). All were stored in a refrigerator until analysis. The certified materials used for evaluation were NCS DC 73349 (bush branches and leaves), CTA-VTL-2 (tobacco leaves), and IAEA-336 (lichen).

Residual water is described as the aqueous fraction of the sludge, a residue of the petrochemical industry. Coming from different sources, this residue is deposited, and water accumulation occurs due to exposure to the environment. This sludge may still contain dissolved solids, metals, oils and resins in lower concentrations. Produced water is an aqueous residue generated in crude oil extraction. The produced water undergoes physical-chemical treatment before final disposal. River water came from the Itajaí-Açu River, located in the southern region of Brazil, in the state of Santa Catarina, where industries from different segments and large cities are concentrated. Drinking water was provided by the local water supply company.

### Preparation of disposable pipette tips

Cork and bract sorbents were prepared according to the method described by Cadorim *et al.*<sup>27</sup> The sorbents were left for 2 h in ultrasonic baths with ultrapure water for cleaning. Then, they were dried in an oven at 110 °C for

12 h, sanded and sieved in a 200  $\mu\text{m}$  mesh. The resulting powder was weighed and added directly into the pipette tips. The cleaning of the sorbent took place prior to use as extraction phase, and the extraction was carried out using seven cycles with 700  $\mu\text{L}$  of 2% solution of  $\text{HNO}_3$  (v/v; 0.44 mol  $\text{L}^{-1}$ ), followed by three cycles with 700  $\mu\text{L}$  ultrapure water.

#### Optimization of procedure for DPX

A  $2^{5-1}$  factorial design with triplicate of the central point was performed to evaluate the influence of the variables: concentration of HCl (1.0, 3.0 and 5.0% v/v), sample pH (2, 5 and 8), extraction phase mass (10, 20 and 30 mg), number of cycles (1, 3 and 5) and NaCl concentration in solution (5, 10 and 15% m/v). The values in parentheses are the minimum, central and maximum levels, respectively. The software used for the evaluation of the experiments was Statistica 13.5,<sup>33</sup> software licensed by the Federal University of Santa Catarina. The response evaluated in this design was the absorbance of Yb. Then, after verifying the significance of the variables, the optimal working conditions were optimized using the response surface methodology, using Box Behnken Design. The minimum, central and maximum levels of the variables were concentration of HCl (1.0, 3.0 and 5.0% v/v), sample pH (2, 5 and 8), and extraction phase mass (10, 20 and 30 mg), and the response considered was the absorbance of Yb. Triplicates were performed with the assistance of multichannel support.

#### Procedure for DPX

All procedures for extraction and pre-concentration of the analyte in the samples follow the same order and involve the following steps: extraction, desorption and cleaning. Initially, the sorbent mass is weighed and inserted into the tip, followed by the conditioning step. The sorbent is cleaned with a suction/discard cycle of 700  $\mu\text{L}$  of acid solution, followed by a cycle of 700  $\mu\text{L}$  ultrapure water. Afterward, the analyte is extracted and pre-concentrated in 5 cycles with 700  $\mu\text{L}$  of individual sample/standard. Desorption of the analyte occurs by applying 1 cycle with 300  $\mu\text{L}$  of HCl 5% v/v solution.

## Results and Discussion

#### Evaluation and characterization of the extraction phase

Initially, different extraction phases (cork, bract, cellulose, phosphate cellulose and chitosan) were evaluated in order to determine which had the best analytical yield. The conditions of sorbent mass, sample pH, number of cycles, solution volumes, analyte concentration and

time in each cycle were fixed, the data are presented in the Supplementary Information (SI) section in Table S1. The results obtained for the initial evaluation of the type of sorbent used in the extraction of Yb by DPX showed that cork provided a greater recovery of the analyte when compared to the other phases. The data are presented in Figure S1 (SI section).

Cork is a material extracted from the bark of *Quercus suber*, and its main composition involves a heterogeneous mixture of suberin (40%) and lignin (24%). Suberin's physicochemical properties focus on hydrophobicity, while lignin provides cell wall resistance. Phenolic groups present in lignin can interact with metals through Lewis acid-base interactions. This type of interaction of phenolic groups and metals gives cork the property of a biosorbent in the extraction of metals in solution.<sup>27,34</sup> However, the binding groups involved in extracting the metals need to be physically available. The preparation of cork took place as described by Cadornim *et al.*,<sup>27</sup> where the cork was reduced to powder and sieved up to a maximum size of 200  $\mu\text{m}$ , facilitating its use as a sorbent and improving physical contact with the sample. Thus, the choice of this biosorbent is due to its ability to extract and pre-concentrate Yb in solution compared to the other phases studied.

The formation of ionic species of Yb in solution was observed by Costa *et al.*,<sup>35</sup> showing that, in solution,  $\text{Yb}^{3+}$  predominates at pH up to around 5.5. After this pH value, the formation of the species  $\text{YbOH}_2^+$  occurs, which predominates at pH above 8.

Cork active sites interact with species with positive charges, as metal ions, and in under certain pH conditions, several species can be formed depending on the buffer used.

Ytterbium metallic speciation ( $2.9 \times 10^{-8}$  mol  $\text{L}^{-1}$ ) in phosphate-buffered solution (0.01 mol  $\text{L}^{-1}$ ) was simulated with the help of Spana software.<sup>36</sup> The diagram is illustrated in SI (Figure S2, SI section). In the pH values between 7.3 and 12.6 there is a predominance of the species  $\text{Yb}(\text{PO}_4)_2^{3-}$ . In the pH range between 8 and 10 is the bioadsorbent action zone of the cork for Yb in a buffered solution with  $\text{PO}_4^{3-}$  (highlighted in a dotted line). This indicates that Yb bioadsorption occurs at positively charged active sites, unlike the results obtained by Cadornim *et al.*,<sup>27</sup> where  $\text{Pb}^{2+}$  and  $\text{Cd}^{2+}$  were bioadsorbed by negatively charged active sites. The versatility of cork can be explained by the different chemical structures present in its composition.

In studies carried out by our research group,<sup>34</sup> using cork as an extractor phase, the chemical and morphological composition of cork were evaluated through analysis of attenuated total reflectance Fourier transform infrared spectroscopy (ATR-FTIR) and energy dispersive X-ray

spectroscopy (EDS).<sup>35</sup> The morphology of recycled cork was also evaluated by scanning electron microscopy (SEM).<sup>27</sup>

According to Mafra *et al.*,<sup>34</sup> the main chemical groups observed in ATR-FTIR include  $\text{C=O}$ ,  $\text{OH}$ ,  $\text{CH}_3$  and  $\text{C=C}$ . The cork used in this work was submitted to ATR-FTIR analysis before and after use as a sorbent, and the results obtained are in agreement with the literature and is presented in the SI section (Figure S3). Also, according to Mafra *et al.*,<sup>34</sup> when subjected to EDS analysis, cork showed a predominant composition of carbon (87.4%), nitrogen (6.0%) and oxygen (6.6%). According to Cadornim *et al.*,<sup>27</sup> the processing of cork for powder reduction allows a porous structure to be obtained, which can promote the physical adsorption of the analyte and, consequently, an increase in the surface area of contact, which influences the analyte/extraction phase interaction.

#### Temperature program optimization for Yb determination

The graphite tube heating program was optimized for the determination of Yb. The pyrolysis and atomization temperatures were evaluated using an aqueous standard solution of Yb  $5 \mu\text{g L}^{-1}$  (mass: 100 pg), without DPX procedure, considering the use of three different permanent modifiers and no modifier. After optimizing the DPX procedure, pyrolysis and atomization curves were performed for an aqueous standard and a sample of residual water, both submitted to the DPX procedure optimized with the modifier selected as optimal. To obtain the pyrolysis and atomization temperature curves, graphite tubes without a PIN platform were used, with and without a permanent chemical modifier. For coating, 20 aliquots with a volume

of  $50 \mu\text{L}$  of each  $1 \text{ g L}^{-1}$  La, W or Zr solution were deposited in each graphite tube according to the standard coating procedure. The curves formed on Yb pyrolysis and atomization with and without the use of a permanent chemical modifier were compared and are shown in Figure 1a. The 2D profile of the analytical signals obtained is shown in Figure 1b.

For the evaluation of pyrolysis and atomization first an aqueous solution of Yb  $5 \mu\text{g L}^{-1}$  was used. The Yb showed significant thermal stability even without chemical modifier. However, significant improvement in the analyte signal acquisition was observed when La was used as a modifier. Compared with the other modifiers (W and Zr) and also without the use of a modifier, La allowed more stable thermal behavior in the pyrolysis and atomization steps. It provided an analytical signal of greater intensity, less tail formation, reduction in analyte atomization time and, in addition, a significant reduction in Yb atomization temperature for this study.

For W, Zr and graphite tube without modifier, the required atomization temperatures were around 2500 to 2600 °C. According to Oliveira *et al.*,<sup>20</sup> the temperature of 2700 °C was ideal for atomizing a  $10 \mu\text{g L}^{-1}$  Yb solution in road dust samples in the presence of  $250 \mu\text{g W}$  as a modifier. For this, Oliveira *et al.*<sup>20</sup> used acid digestion with  $\text{HNO}_3$ , which can favor the formation of refractory species and hinder the atomization of the analyte. These atomization temperatures are too high and cause significant wear in graphite tubes. The use of lower temperatures provides a longer lifespan for the graphite tube, without harming the analytical results obtained.

Elevated temperatures in the pyrolysis step can reduce possible interferences present in the matrix. In Figure 1a, it

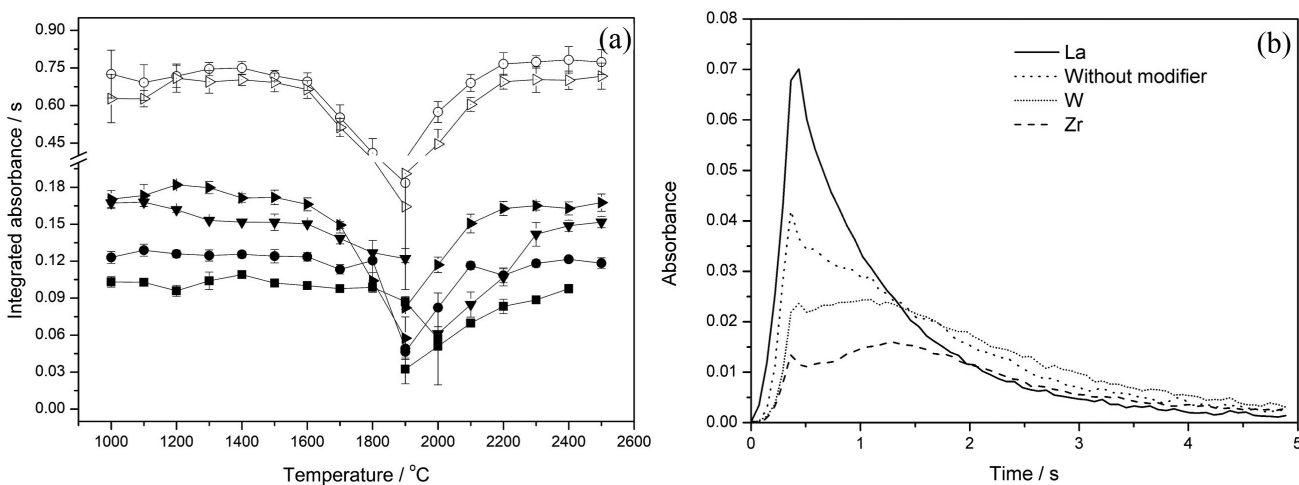


**Figure 1.** Pyrolysis and atomization curves for Yb determination by HR-CS GF AAS. (a) The pyrolysis and atomization curves for aqueous standard Yb  $5.0 \mu\text{L}^{-1}$  without DPX, (-●-) without modifier, with permanent chemical modifiers (-■-) Zr, (-▶-) La, (-▼-) W, aqueous standard Yb  $5.0 \mu\text{L}^{-1}$  with DPX + La (-○-) and residual water with DPX + La (-▷-); (b) 2D profiles analytical signals obtained for the aqueous standard Yb  $5.0 \mu\text{L}^{-1}$  without DPX. Pyrolysis temperatures ( $T_{\text{pyr}}$ ) of 1400 °C and atomization temperature ( $T_{\text{atom}}$ ) of 2500 °C were fixed for the optimizations.

is also shown the thermal behavior of an aqueous solution and a sample of residual water, both submitted to the optimized DPX procedure, which will be detailed in the next sub-sections. It can be observed that similar thermal behavior was observed, the gain in sensitivity inherent to the pre-concentration procedure is perceived. The sample goes through a DPX preparation process that promotes the elimination or reduction of interfering elements. Thus, lower pyrolysis temperatures can be applied without impairing the analysis. La allowed the use of  $T_{\text{pyr}}$  1400 °C and  $T_{\text{atom}}$  2400 °C, obtaining more intense analytical signals. Furthermore, the peak profile in the Yb atomization with and without the use of DPX and acid solution in the desorption remained without significant changes. Therefore, La was selected as a permanent chemical modifier in the following experiments.

#### DPX condition optimization

##### Evaluation of cleaning and desorption solutions

The extractor phase cleaning and analyte desorption steps are critical to avoid memory effects or sorbent saturation by the analyte. Thus, evaluations were made regarding the use of acidic solutions in both steps used in DPX with cork as a sorbent. Solutions of HNO<sub>3</sub>, HCl and H<sub>2</sub>SO<sub>4</sub> (5%, v/v) acids were used. A 5 µg L<sup>-1</sup> Yb solution was used in the extraction step. The other variables were kept constant: sorbent mass, sample pH, number of cycles, solution volumes and time in each cycle are presented in the SI section (Table S1). Table 3 presents the mean values obtained for 3 extraction cycles (n = 3).

**Table 3.** Evaluation of the use of acids in the cleaning and desorption steps for Yb 5 µg L<sup>-1</sup> with DPX by HR-CS GF AAS (n = 3)

Extractor phase cleaning	Analyte desorption	Average (Abs <sub>m</sub> )	SD	RSD / %
HNO <sub>3</sub>	HNO <sub>3</sub>	0.1645	0.0037	2.28
HNO <sub>3</sub>	HCl	0.2349	0.0153	6.53
HCl	HNO <sub>3</sub>	0.1089	0.0028	2.64
HCl	HCl	0.2211	0.0079	3.60
HNO <sub>3</sub>	H <sub>2</sub> SO <sub>4</sub>	0.0843	0.0024	2.84

Abs<sub>m</sub>: integrated absorbance; SD: standard deviation; RSD: relative standard deviation.

The evaluation of the results obtained for the extractor phase cleaning and analyte desorption steps indicates that the use of HNO<sub>3</sub> in the cleaning step and HCl in the desorption step promoted a higher yield in the extraction of Yb when compared to other conditions. However, the use of HNO<sub>3</sub> in the desorption step promoted a reduction

in the signal, while HCl increased the signal. HNO<sub>3</sub> in the desorption step can lead to the formation of refractory oxides and reduce analyte atomization. In contrast to this, the use of HCl can favor the formation of more volatile Yb halides. The use of HCl/HCl in both steps has a value significantly the same ( $t_{\text{cal}} = 1.37 < t_{\text{crit}} = 2.78$ ) as that obtained with the use of HNO<sub>3</sub>/HCl, but with a lower relative standard deviation (RSD, in percentage). Thus, the combination of HCl/HCl in the two stages is more suitable for DPX with cork, which was selected for the experiments.

##### Univariate evaluation of extraction time

After the selection of the sorbent, temperatures and acid, the influence of the extraction time in each cycle was evaluated through a univariate experiment. The evaluation of the extraction time or interaction with the sorbent is very important to measure the balance between the phases and the analyte. The extraction time is the ratio between the time spent by the analyte in aqueous solution and in contact with the solid extracting phase, which directly influences its pre-concentration and extraction. Thus, the times of 1, 15 and 30 s in the Yb 5 µg L<sup>-1</sup> extractions with five cycles each were evaluated. The results are shown in the Figure S4 (SI section).

Based on the results obtained, the *t* test (95% confidence) was applied, and the results with cycles of 1 s showed no significant difference in analyte extraction when compared with time of 15 s ( $t_{\text{cal}} = 0.79 < t_{\text{crit}} = 4.31$ ), considering the averages with different variances ( $F_{\text{cal}} = 40.29 > F_{\text{crit}} = 19.0$ ), degree of freedom equal to 2. Comparing the times of 1 and 30 s, averages with same variance ( $F_{\text{cal}} = 12.56 < F_{\text{crit}} = 19.00$ ), degree of freedom equal to 4, there is significant difference ( $t_{\text{cal}} = 10.13 > t_{\text{crit}} = 2.77$ ). And for the times 15 and 30 s, averages with same variance ( $F_{\text{cal}} = 3.21 < F_{\text{crit}} = 19.00$ ), degree of freedom equal to 4, there is also a significant difference ( $t_{\text{cal}} = 4.44 > t_{\text{crit}} = 2.77$ ). It was observed that the use of times of 15 and 30 s associated with 5 extraction cycles did not favor the pre-concentration and extraction of Yb. A possible cause of this result may be related to the equilibrium formed between the extraction phase, analyte and the solution. Over time, Yb returns to the solution through the possibility of back-extraction, since the solution would be more diluted. So, cycles of 1 s extraction were selected as the optimized condition.

##### Multivariate evaluations

The selection of significant factors was based on Pareto plot studies and univariate evaluations of experiments for some predefined conditions. It was considered that each cycle involves the steps of aspiration of the solution with

air, a waiting time interval and, subsequently, the disposal of the solution. The set of cycles involving extraction, desorption and cleaning comprises the process of extracting the analyte from the sample; thus, an extraction cycle. All optimization DPX experiments were performed using a  $5 \mu\text{g L}^{-1}$  Yb solution.

The efficiency of the developed method can be affected by some parameters. In order to obtain a higher yield in the extraction and concentration of the analyte, five variables were evaluated in a multivariate design. Concentration of HCl for desorption (1.0, 3.0 and 5.0% v/v), sample pH (2, 5 and 8), extraction phase mass (10, 20 and 30 mg), number of cycles (1, 3 and 5) and NaCl concentration in solution (5, 10 and 15% m/v), as well as the interaction between these factors, were evaluated. From a  $2^{5-1}$  factorial design, a Pareto chart was obtained with the predominant factors shown in Figure 2.

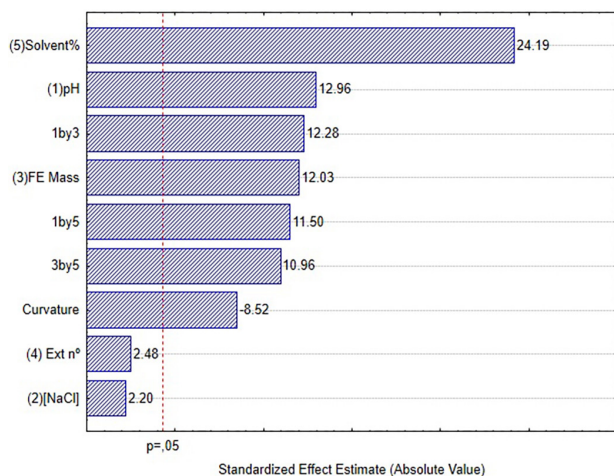


**Figure 2.** Pareto chart obtained by a  $2^{5-1}$  factorial design, evaluation of parameters of the: (1) pH; (2) NaCl concentration in solution; (3) extractor phase mass; (4) number of extractions and (5) solvent percentage.

The results obtained show that there is a significant influence of the concentration of HCl as solvent in the desorption, pH of the sample and mass of the extraction phase in the extraction of the analyte in solution. All these significant factors showed positive effect values, indicating that the closer to the maximum level of these variables, the greater the extraction of Yb. However, the number of cycles and the % m/v of NaCl are not significant under the evaluated conditions. Thus, the number of cycles was fixed at 3, the central point condition, and the concentration of NaCl in solution was removed for the following experiments. The curvature that allows the quality of the levels studied in the planning to be evaluated as a region tending to the maximum response was significant, but with a negative effect, indicating that for a response surface methodology, an adjustment in the minimum, maximum

and central levels is necessary so that it is possible to obtain a maximum surface.

The optimization of the parameters of sample pH and HCl concentration (% v/v) in desorption was selected for further studies based on the results obtained in the Pareto chart. The Doehlert matrix was used with methodology response surface. Thus, for the evaluation of these parameters, the pH of the sample was varied by 7, 8 and 9, and the HCl% by 2.0, 3.5, 5.0, 6.5 and 8.0% v/v. The extracting phase mass was fixed in 20 mg. The response surfaces obtained for the Doehlert matrix did not provide a well-defined maximum, but a saddle point surface, indicating the need to expand the range levels of the factors to better observe the behavior of the analyte for mathematical modeling. Experimentally this is a challenge, as the extraction phase tends to decompose at a higher pH (close to 11). However, the results indicated that high pH may have provided better extractions. A possible explanation would be related to the low concentration of Yb in solution used,  $5 \mu\text{g L}^{-1}$ , and the interaction sites of the extraction phase. Species of hydroxy complexes can be formed in a solution starting from pH 5.5,<sup>35</sup> but due to the low concentration of Yb, the occurrence of precipitation of this hydrolyzed metal is not possible. Hydrolyzed and negatively charged species of Yb can interact more strongly with positively charged groups present in the cork structure after conditioning with HCl.

Considering improving mathematical modeling, another response surface methodology was chosen, since in the Pareto chart the extraction phase mass was a significant factor. A Box Behnken design was carried out for the three variables: sample pH (4.0, 8.0 and 12.0), the concentration of HCl for desorption (2.0, 4.0 and 6.0% v/v), and extraction phase mass (10, 15 and 20 mg). The results obtained on the response surfaces of the Box Behnken design are shown in Figures 3a, 3b and 3c.

The surfaces indicate a well-defined maximum region, especially on the pH  $\times$  HCl% and pH  $\times$  mass surfaces. The analysis of variance indicates that there was no lack of fit and that 96.5% of the data was explained by the model. It can be seen that there is a wide range of pH values, which favors a good extraction of the analyte. However, the extraction phase tends to decompose at a higher pH. Considering the visual inspection of the surface, the optimal conditions were pH 8.0, concentration of HCl 5% v/v and extraction phase mass of 20 mg.

#### Interference assessment

The use of DPX as an extraction and pre-concentration method provides some advantages such as matrix exclusion and analyte selection. However, the extraction can be

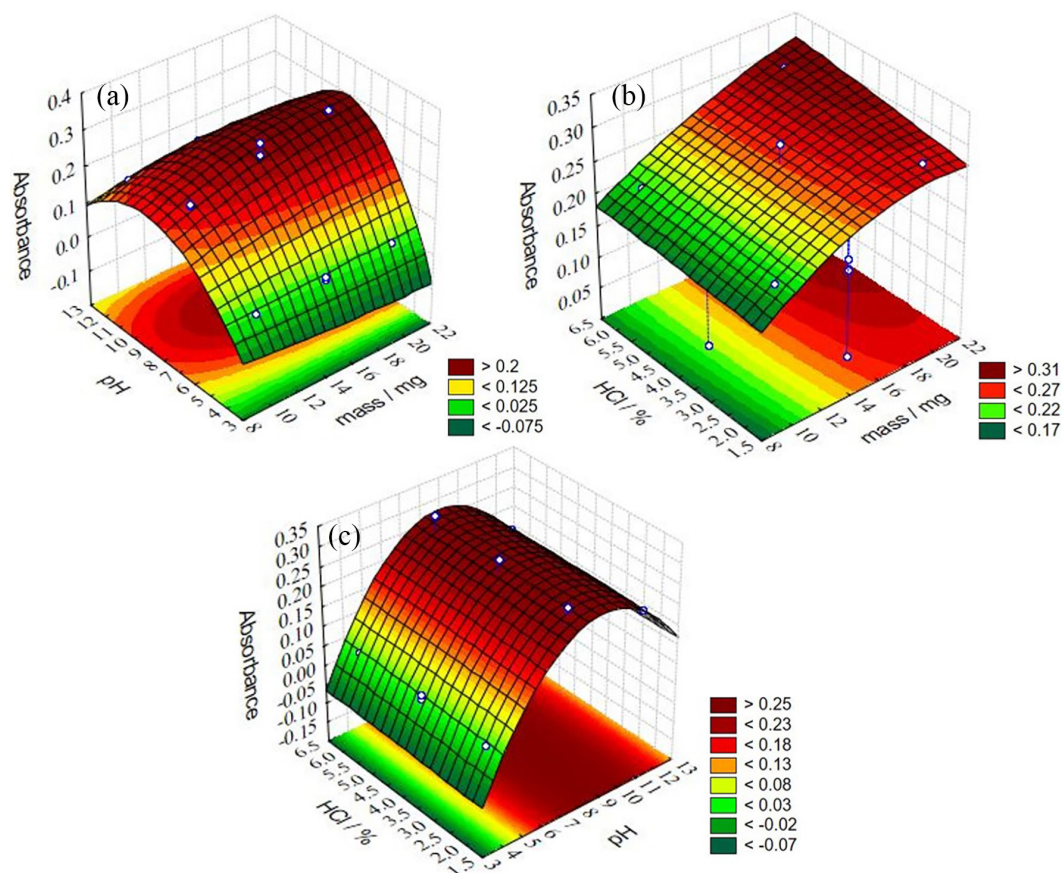


**Figure 3.** Box Behnken obtained for correlation (a) pH and mass (mg); (b) HCl (% v/v) and mass (mg); (c) HCl (% v/v) and pH.

influenced by the presence of other ions that compete by the active sites present in the sorbent structure. Competition for the active sites of the sorbent can reduce the efficiency of the method and cause loss of accuracy if proper care is not taken with the method.

Some cations and anions are known to be abundant in wastewater and natural water and are often present in the most diverse industrial segments, as is the case of  $\text{Na}^+$ ,  $\text{K}^+$ ,  $\text{Ca}^{2+}$ ,  $\text{Mg}^{2+}$ ,  $\text{Al}^{3+}$ ,  $\text{NO}_3^-$ ,  $\text{SO}_4^{2-}$ ,  $\text{Cl}^-$ ,  $\text{C}_2\text{O}_4^{2-}$ , and  $\text{CH}_3\text{COO}^-$ .<sup>37-39</sup> Thus, the evaluation of possible interferences present in the matrix was carried out taking these species into account. Good recoveries were considered within the range of 80-120%. Table 4 presents the maximum recovery values obtained for Yb and interferences.

The results obtained for nitrate and chloride salts containing  $\text{Na}^+$ ,  $\text{K}^+$ ,  $\text{Mg}^{2+}$  and  $\text{Ca}^{2+}$  cations showed a similar behavior. The maximum concentration with acceptable recovery for these ions was 2000 times greater than that of Yb in solution, indicating that competition for cork active sites can occur at higher concentrations of interferences. However, for the nitrate salt containing  $\text{Al}^{3+}$  the maximum concentration with acceptable recovery was 100 times the concentration of Yb in solution. A possible explanation for this is the competition between  $\text{Al}^{3+}$  and  $\text{Yb}^{3+}$  in the

**Table 4.** Influence of matrix ions on the recoveries of Yb ( $5 \mu\text{g L}^{-1}$ ) using the DPX-cork technique

Added salt	Yb		
	Maximum concentration / ( $\text{mg L}^{-1}$ )	Ratio [ion]/[Yb]	Recovery / %
NaCl	10	2000	99.8
KCl	10	2000	94.2
$\text{CaCl}_2$	10	2000	105.1
$\text{Mg}(\text{NO}_3)_2$	10	2000	105.2
$\text{Al}(\text{NO}_3)_3$	0.5	100	86.6
$\text{NaNO}_3$	5	1000	80.7
$\text{C}_2\text{H}_3\text{NaO}_2$	15	3000	88.1
$\text{Na}_2\text{SO}_4$	0.5	100	< 80
$\text{Na}_2\text{C}_2\text{O}_4$	0.5	100	95.3

phosphate buffered solution, reducing the presence of Yb in the active sites of cork.

$\text{Al}^{3+}$  showed greater interaction when compared to the other cations. This interaction may be related to the ion charge. However, for higher concentrations of cations with high oxidation number as well as a higher pH value, precipitation of certain cations may occur. This effect



caused by the use of higher pH associated with DPX favors the precipitation of interferents. Furthermore, the formed precipitate can be retained in the analyte extraction step and excluded along with the matrix.

For  $\text{NaNO}_3$ , the maximum concentration with acceptable recovery was 1000 times the Yb concentration. In this case, it is likely that the saturation of the extracting phase will occur through excess salt, preventing the analyte from being properly extracted.

For anions, it was observed that chloride and nitrate salts ( $\text{CaCl}_2$  and  $\text{Mg}(\text{NO}_3)_2$  up to 4000 times) did not have a significant influence on the concentration of Yb in solution. In contrast, the evaluated sulfate ( $\text{Na}_2\text{SO}_4$ ) presented a lower maximum concentration of recovery (100 times) compared to the concentration of Yb. Sulfates have a good affinity for REE metals and can compete with phosphates for the analyte. Thus, the low recovery associated with sulfate may be related to competition between this salt and phosphate for Yb.

For sodium acetate and sodium oxalate anions, which are organic salts, it was observed that sodium acetate showed similar behavior to chloride and nitrate salts, and the maximum recovery concentration was 3000 times that of Yb. For sodium oxalate, increasing the concentration of this salt in solution may interfere with Yb recovery more sharply when compared to sodium acetate. Thus, the maximum concentration for recovery was 100 times the concentration of Yb. Oxalates are often used as complexing agents for REEs and other metals, which may interfere with the adsorption of the analyte.<sup>37</sup>

#### Figures of merit

Figures of merit, limit of quantification (LOQ), limit of detection (LOD), coefficient of determination ( $R^2$ ), enrichment factor, linear range, characteristic mass and curve equation for Yb using DPX as the preparation method were determined. The values for absolute LOD and LOQ were calculated as 3 and 10  $\sigma/S$  ( $n = 10$ ), respectively, where  $\sigma$  is the standard deviation of a blank sample and  $S$  is the slope of the calibration curve. The data are presented in Table 5 and Figure S5 (SI section).

The enrichment factor was calculated through the ratio between the calibration curves with and without DPX. For the proposed extraction and pre-concentration method for Yb, an enrichment factor of 4 was obtained. This parameter can be used to evaluate the performance of the analytical method compared to other methods. In addition, it is possible to evaluate the performance for the determination of species of interest at relatively low concentrations, providing an improvement in LOD.<sup>40</sup> In the literature, enrichment factors by the DPX method of 12

**Table 5.** Figures of merit for the DPX method applied to the determination of Yb in environmental samples by the HR-CS GF AAS technique

Parameter	Value
LOD relative / ( $\mu\text{g L}^{-1}$ )	0.03
LOQ relative / ( $\mu\text{g L}^{-1}$ )	0.01
LOD absolute / pg	0.072
LOQ absolute / pg	0.021
Characteristic mass / pg	0.6
$R^2$	0.9961
Curve equation	$y = 0.1467x + 0.0014$
Linear range / ( $\mu\text{g L}^{-1}$ )	0.5-5
Enrichment factor	4

LOD: limit of detection; LOQ: limit of quantification;  $R^2$ : coefficient of determination.

and 50 for Cr and Cu, respectively, have been reported with subsequent determination via FAAS.<sup>28,40</sup> The enrichment factor obtained by the DPX method in this study was satisfactory for Yb.

The values obtained from the calibration curve was LOQ  $0.03 \mu\text{g L}^{-1}$ , LOD  $0.01 \mu\text{g L}^{-1}$  and  $R^2$  0.9961. Comparing the values obtained for the LOQ and LOD with the values reported in the literature using sample preparation methods, it was found that the proposed method meets the feasibility requirements. Table 6 presents the values found in the literature in the determination of Yb.

The values reported by Oliveira *et al.*,<sup>20</sup> are two larger orders using the same determination technique and with ultrasound sample preparation. Furthermore, the pyrolysis and atomization temperatures using W as modifier are 1500 and 2700 °C, much higher than those obtained using La as chemical modifier at 1400 and 2400 °C, respectively. Also, the time required for preparation was 34 times shorter when compared with the use of multichannel support.

Only methods employing ICP obtained similar results for LOQ and LOD. However, these methods require more sample preparation and some use complex chemical modifiers. Consequently, the costs associated with each method are comparatively higher. All methods employing the ICP technique present longer execution times than those used in DPX by HR-CS GF AAS.

Application of DPX in environmental samples in the determination of Yb by HR-CS GF AAS

#### Accuracy evaluation

The evaluation of the accuracy of the method was performed by applying three CRMs, NCS DC 73349

**Table 6.** Comparison of methods reported in the literature for the determination of Yb and/or REE using sample preparation methods

Analyte	Sample	Technique	Method	Extraction phase	Modifier	Reagents	Limits of detection and quantification	Reference
Yb	road dust	HR-CS GF AAS	sonication	HNO <sub>3</sub>	W	HNO <sub>3</sub> 0.24 mol L <sup>-1</sup>	LOD 0.11 µg L <sup>-1</sup>	20
Gd, La, Tb, Tm, Yb and Y	geological and catalyst	ETV-ICP-MS	DLLME	CHCl <sub>3</sub> and 8-hydroxyquinoline	Pd	HNO <sub>3</sub> , HCl, H <sub>2</sub> O <sub>2</sub> , HF and H <sub>3</sub> BO <sub>3</sub>	LOD 0.1 ng g <sup>-1</sup>	41
Y, La, Ce, Pr, Nd, Sm, Eu, Gd, Tb, Dy, Ho, Er, Tm, Yb and Lu	environmental water and sediment	ETV-ICP-MS	D-SPE-DLLME	Chelex 100, CCl <sub>4</sub>	PMBP	0.1 mol L <sup>-1</sup> HNO <sub>3</sub> / 125 mmol L <sup>-1</sup> Tris	LOD 0.008 ng L <sup>-1</sup>	42
La, Ce, Pr, Nd, Sm, Eu, Gd, Tb, Dy, Ho, Er, Tm, Yb and Lu	mineral water, from river and from reference	ICP-OES	CPE	Triton X-114 and TTA			LOD 0.002 µg L <sup>-1</sup>	43
Nd, Sm, Eu, Gd, Tb, Dy, Ho, Yb, Lu and Ce	water	ICP-OES	SPE	functionalized Amberlite XAD-4 resin		HNO <sub>3</sub> 0.24 mol L <sup>-1</sup>	LOD 0.006 µg L <sup>-1</sup>	44
Yb	natural, potable, produced water and liquid waste	HR-CS GF AAS	DPX	cork	La	HCl 5%	LOQ 0.03 µg L <sup>-1</sup> LOD 0.01 µg L <sup>-1</sup>	this work

LOD: limit of detection; LOQ: limit of quantification; LLE: liquid-liquid extraction; DLLME: dispersive liquid-liquid micro extraction; D-SPE: dispersive solid phase extraction; CPE: cloud point extraction; SPE: solid phase extraction; Triton X-114: octylphenoxypolyethoxyethanol; TTA: 1-(2-thenoyl)-3,3,3-trifluoroacetone; PMBP: 1-phenyl-3-methyl-4-benzoylpyrazolone; TODGA: *N,N,N',N'*-tetraoctyl dilicholamide; DEHPA: di-(2-ethylhexyl)phosphoric acid; ETV-ICP-MS: electrothermal vaporization-inductively coupled plasma-mass spectrometry; ICP-OES: inductively coupled plasma optical emission spectrometry; HR-CS GF AAS: high-resolution continuum source graphite furnace atomic absorption spectrometry.

(bush branches and leaves), CTA-VTL-2 (tobacco leaves), and IAEA-336 (lichen). The CRMs were digested in a microwave oven using acidic solution, and the resulting solution was subjected to Yb analysis by the ICP-MS technique. The values obtained by ICP-MS are in accordance with the values reported for the CRMs. After that, the solutions were subjected to pH adjustment and applied to the DPX method for Yb determination by HR-CS GF AAS. The results obtained are shown in Table 7.

The *t* test of means comparison was applied, and the values obtained from the *t* calculated for the samples, considering the results of the ICP-MS and the proposed method, were lower than the critical *t* for 95% confidence (2.776) for samples NCS DC 73349 and CTA-VTL-2. The difference was significant only for the IAEA-336 sample, because the result of the ICP-MS was higher than expected, a possibility of interference. Considering the values reported as a reference, the calculated *t* values were lower than the critical *t* (4.313) for a 95% confidence level, indicating that

**Table 7.** Comparison of determination of Yb in samples and CRMs by ICP-MS and HR-CS GF AAS DPX-cork. The values represent the mean of three measurements ± standard deviation

Sample	Yb				
	Found ICP-MS / (µg g <sup>-1</sup> )	Found HR-CS GF AAS DPX-cork / (µg g <sup>-1</sup> )	<i>t</i> <sup>a</sup>	Reference / (µg g <sup>-1</sup> )	<i>t</i> <sup>b</sup>
NCSDC 73349	0.065 ± 0.010	0.060 ± 0.004	0.804	0.063 ± 0.009 <sup>c</sup>	1.299
CTA-VTL-2	0.083 ± 0.005	0.075 ± 0.005	1.960	0.080 <sup>d</sup>	1.732
IAEA-336	0.041 ± 0.002	0.034 ± 0.003	3.363	0.037 <sup>d</sup>	1.732
Residual water	< LOQ <sup>e</sup>	< LOQ <sup>f</sup>			
Produced water	< LOQ <sup>e</sup>	< LOQ <sup>f</sup>			
Drinking water	< LOQ <sup>e</sup>	< LOQ <sup>f</sup>			
River water	< LOQ <sup>e</sup>	< LOQ <sup>f</sup>			

<sup>a</sup>Means comparison method; <sup>b</sup>mean comparison with a known value method; <sup>c</sup>certificate; <sup>d</sup>value informed; <sup>e</sup>ICP-MS LOQ: 0.015 µg L<sup>-1</sup>; LOD: 0.009 µg L<sup>-1</sup>; <sup>f</sup>HR-CS GF AAS LOQ: 0.03 µg L<sup>-1</sup>; LOD: 0.01 µg L<sup>-1</sup>.

there was no significant difference between the values obtained by the proposed methodology and the reported values.

The spectra obtained for an IEAE-336 CRM solution digested in a microwave oven, with an integration time of 5.0 s, free of interference close to the spectral line used for Yb, are shown in Figures 4A and 4B. In both spectra it is possible to observe the presence of Ti in another absorption region. The presence of Ti does not interfere in the determination of Yb. However, it was observed that the signal for Ti also increases when using the DPX method. Possibly the simultaneous extraction of Ti occurs, at a lower percentage.

#### Precision assessment and analysis of environmental samples

As it is a new methodology, the efficiency of Yb extraction and pre-concentration using DPX was evaluated

in a wide variety of environmental samples. The studied environmental and wastewater samples present high chemical and physical complexity, each one presenting different characteristics.

The evaluation of the proposed method was applied to samples of drinking water, river water, produced water and residual water. The samples used in the study were previously analyzed using the ICP-MS and HR-CS GFAAS and did not present Yb in solution (Table 7). For this study, samples were enriched with three different concentrations (1, 3 and 5  $\mu\text{g L}^{-1}$  of Yb) the results are shown in Table 8. The recovery was more effective for the aqueous phase of the residual and for drinking water, with recovery values close to 100%.

These low interval recovery results for river water can be associated with quantities of tailings containing complexing agents from the disposal of adjacent sewage

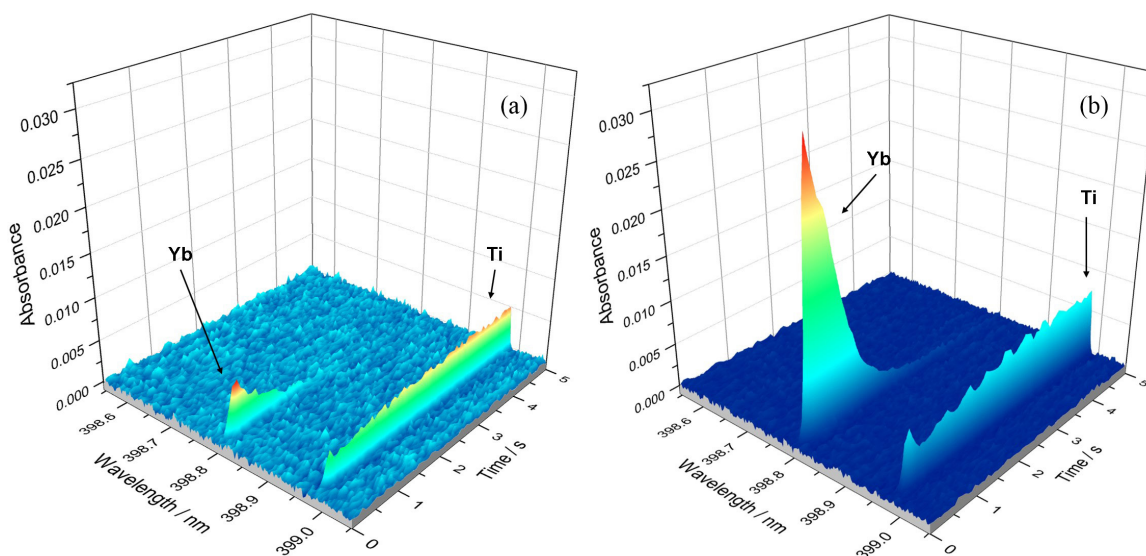


**Figure 4.** Comparison of temporally resolved absorption spectra in the vicinity of the Yb analytical line at 398.799 nm, with 1000  $\mu\text{g}$  of La as permanent chemical modifier and detection by HR-CS-GF AAS: (a) direct analysis of digested CRM IEAE-336 (b) analysis using DPX-cork.

**Table 8.** Application of DPX for the recovery of Yb in environmental samples (n = 3)

Sample	Yb / ( $\mu\text{g L}^{-1}$ )	Average (Abs <sub>int</sub> )	SD	RSD / %	Value obtained	REC / %
Residual water	1	0.15701	0.00485	3.1	1.1	108.2
	3	0.46863	0.02217	4.7	3.2	107.1
	5	0.71591	0.01404	2.0	4.9	98.0
Produced water	1	0.11118	0.01538	13.8	0.8	76.9
	3	0.16922	0.01525	9.0	1.2	38.8
	5	0.24182	0.01059	4.4	1.7	33.2
Drinking water	1	0.16060	0.00855	5.3	1.1	110.6
	3	0.42956	0.00223	0.5	2.9	98.2
	5	0.61845	0.02104	3.4	4.2	84.7
River water	1	0.13511	0.00596	4.4	0.9	93.2
	3	0.31587	0.00341	1.1	2.2	72.3
	5	0.47148	0.02715	5.8	3.2	64.6

Abs<sub>int</sub>: integrated absorbance; SD: standard deviation; RSD: relative standard deviation; REC: recovery.

treatment plants. Likewise, when the recoveries for produced water are observed, the results are lower. The produced water comes from underground formations brought to the surface together with oil and generated as a by-product of petrochemical production. The chemical composition of produced water can vary greatly depending on the origin of the oil source.<sup>45</sup> These low recovery results may be associated with the physicochemical characteristics of these matrices. According to Cadornim *et al.*,<sup>27</sup> the percentage of recovery of analytes (Cd and Pb) using the DPX extraction method varied according to the sample dilution. For a sample of undiluted seawater, the recoveries were 40% for Cd and 45% for Pb, with a 1:2 dilution these values increased to 50 and 62% and with a 1:5 dilution both obtained 90%, respectively. The samples evaluated in this study were not diluted, and for higher Yb concentrations, the interference caused by the matrix may be more prominent. In this way, the DPX method presented excellent results for residual water and drinking water without the use of dilution, in both samples the recoveries were satisfactory, staying within the limits of 80 to 120%.

## Conclusions

The DPX method developed for the extraction and pre-concentration of Yb combined with the determination by HR-CS GF AAS in residual water was considered satisfactory. The use of disposable tips with biosorbent material (cork) proved to be easy to perform and prepare and incurred a low cost. The data obtained show that the method has good reproducibility and repeatability for different interfering ions, as well as analytical performance. The extraction and pre-concentration of Yb were satisfactory using different aliquots in the process. In addition, DPX provides for the cleaning of the aqueous matrix loaded with suspended materials from the filtration, retaining the analyte in its structure. The limits of quantification and detection were lower than those reported in the literature by up to two orders. The limits of quantification, detection, accuracy and precision of the method were satisfactory. In addition, the proposed method allowed the use of a reduced volume of acid solution (300  $\mu$ L), extractor phase mass (20 mg) and an easy sample preparation step. It can be applied in different aqueous matrices.

## Supplementary Information

Supplementary information is available free of charge at <http://jbcs.sbcs.org.br> as a PDF file.

## Acknowledgments

The authors are grateful to the Conselho Nacional de Desenvolvimento Científico e Tecnológico, CNPq, Brazil and the Coordenação de Aperfeiçoamento de Pessoal de Nível Superior, CAPES, Brazil for scholarships and financial support.

## References

1. da Costa, T. B.; da Silva, M. G. C.; Vieira, M. G. A.; *J. Rare Earths* **2020**, *38*, 339. [Crossref]
2. Du, X.; Graedel, T. E.; *Environ. Sci. Technol.* **2011**, *45*, 4096. [Crossref]
3. Charalampides, G.; Vatalis, K. I.; Apostoplos, B.; Ploutarch-Nikolas, B.; *Procedia Econ. Financ.* **2015**, *24*, 126. [Crossref]
4. Rodrigues, E. S.; Montanha, G. S.; Marques, J. P. R. M.; Almeida, E.; Yabuki, L. N. M.; Menegário, A. A.; Carvalho, H. W. P.; *J. Rare Earths* **2020**, *38*, 1131. [Crossref]
5. Zheng, Z.; Xiong, C.; *J. Rare Earths* **2011**, *29*, 407. [Crossref]
6. Ahmad, H.; Ahmed, M. H. M.; Yusoff, N.; Ramli, R.; Samion, M. Z.; *Opt. Laser Technol.* **2020**, *130*, 106350. [Crossref]
7. Ahmad, G. N.; Raza, M. S.; Singh, N. K.; Kumar, H.; *Opt. Laser Technol.* **2020**, *126*, 106117. [Crossref]
8. Zhou, R.; Tong, D. G.; *Ind. Eng. Chem. Res.* **2020**, *86*, 211. [Crossref]
9. Zhang, P.; Qin, H.; Lv, W.; Zhang, H.; Hu, J.; *Sens. Actuators, B* **2017**, *246*, 9. [Crossref]
10. Brova, M. J.; Alat, E.; Pauley, M. A.; Sherbondy, R.; Motta, A. T.; Wolfe, D. E.; *Surf. Coat. Technol.* **2017**, *331*, 163. [Crossref]
11. Sundaresan, P.; Krishnapandi, A.; Chen, S.-M.; *J. Taiwan Inst. Chem. Eng.* **2019**, *96*, 509. [Crossref]
12. Xin, X.; Zhang, M.; Ji, S.; Dong, H.; Zhang, L.; *J. Solid State Chem.* **2018**, *262*, 186. [Crossref]
13. Tcibulnikova, A. V.; Slezhkin, V. A.; Bruykhhanov, V. V.; Samusev, I. G.; Kozhevnikov, A. S.; Savin, V. V.; Medvedskaya, P. N.; Lyatun, I. I.; *Opt. Commun.* **2020**, *459*, 125006. [Crossref]
14. Li, F.-K.; Gong, A.-J.; Qiu, L.-N.; Zhang, W.-W.; Li, J.-R.; Liu, Y.; Li, J.-D.; Gao, G.; Yuan, X.-T.; *Microchem. J.* **2019**, *147*, 93. [Crossref]
15. Harbison, R.; Bourgeois, M.; Johnson, G.; *Hamilton & Hardy's Industrial Toxicology*, 6<sup>th</sup> ed.; John Wiley & Sons, Inc.: Hoboken, USA, 2015.
16. Pagano, G.; *Rare Earth Elements in Human and Environmental Health: At the Crossroads Between Toxicity and Safety*, 1<sup>st</sup> ed.; Jenny Stanford Publishing: New York, USA, 2016. [Crossref]
17. Zawisza, B.; Pytlakowska, K.; Feist, B.; Polowniak, M.; Kita, A.; Sitko, R.; *J. Anal. At. Spectrom.* **2011**, *26*, 2373. [Crossref]
18. Fisher, A.; Kara, D.; *Anal. Chim. Acta* **2016**, *935*, 1. [Crossref]
19. Wysocka, I.; *Talanta* **2021**, *221*, 121636. [Crossref]

20. Oliveira, S. S.; Ribeiro, V. S.; Almeida, T. S.; Araujo, R. G. O.; *Spectrochim. Acta, Part B* **2020**, *171*, 105938. [Crossref]
21. Goltz, D. M.; Grégoire, D. C.; Chakrabarti, C. L.; *Spectrochim. Acta, Part B* **1995**, *50*, 1365. [Crossref]
22. Aghabalazadeh, S.; Ganjali, M. R.; Norouzi, P.; *Spectrosc. Lett.* **2016**, *49*, 491. [Crossref]
23. Khan, W. A.; Arain, M. B.; Soylyak, M.; *Food Chem. Toxicol.* **2020**, *145*, 111704. [Crossref]
24. Kabeer, M.; Hakami, Y.; Asif, M.; Alrefaei, T.; Sajid, M.; *TrAC, Trends Anal. Chem.* **2020**, *130*, 115987. [Crossref]
25. Feist, B.; Sitko, R.; *Microchem. J.* **2019**, *147*, 30. [Crossref]
26. Anthemidis, A. N.; Adam, I. S. I.; *Anal. Chim. Acta* **2009**, *632*, 216. [Crossref]
27. Cadornim, H. R.; Schneider, M.; Hinz, J.; Luvizon, F.; Dias, A. N.; Carasek, E.; Welz, B.; *Anal. Lett.* **2019**, *52*, 2133. [Crossref]
28. Tomasin, G. S.; Silva, W. R.; Costa, B. E. S.; Coelho, N. M. M.; *Microchem. J.* **2021**, *161*, 105749. [Crossref]
29. Corazza, G.; Merib, J.; do Carmo, S. N.; Mendes, L. D.; Carasek, E.; *J. Braz. Chem. Soc.* **2019**, *30*, 1211. [Crossref]
30. Huelsmann, R. D.; Will, C.; Carasek, E.; *Talanta* **2021**, *221*, 121443. [Crossref]
31. Heitmann, U.; Becker-Ross, H.; Florek, S.; Huang, M.; Okruss, M.; *J. Anal. At. Spectrom.* **2006**, *21*, 1314. [Crossref]
32. Kim, S. G.; Choi, H. J.; Jhon, M. S.; *Macromol. Chem. Phys.* **2001**, *202*, 521. [Crossref]
33. *Statistica (data analysis software system)*, version 13.5; StatSoft, Inc., California, USA, 2022. [Link] accessed in January 2023
34. Mafra, G.; Spudeit, D.; Brognoli, R.; Merib, J.; Carasek, E.; *J. Chromatogr. B: Anal. Technol. Biomed. Life Sci.* **2018**, *1102-1103*, 159. [Crossref]
35. da Costa, T. B.; ds Silva, M. G. C.; Vieira, M. G. A.; *J. Cleaner Prod.* **2021**, *279*, 123555. [Crossref]
36. Puigdomenech, I.; *Spana*, version 2020-June-08; KTH Royal Institute of Technology, Sweden, 2022.
37. Fa, Y.; Yu, Y.; Li, F.; Du, F.; Liang, X.; Liu, H.; *J. Chromatogr. A* **2018**, *1554*, 123. [Crossref]
38. Lv, T.-T.; Ma, W.; Zhang, D.; Zhang, T.; Tang, J.-H.; Zeng, X.; Feng, M.-L.; Huang, X.-Y.; *Chem. Eng. J.* **2022**, *435*, 134906. [Crossref]
39. Yan, Y.; Wan, B.; Mansor, M.; Wang, X.; Zhang, Q.; Kappler, A.; Feng, X.; *Sci. Total Environ.* **2022**, *803*, 149918. [Crossref]
40. Silva, W. R.; Costa, B. E. S.; Batista, A. D.; Alves, V. N.; Coelho, N. M. M.; *J. Braz. Chem. Soc.* **2022**, *33*, 498. [Crossref]
41. Ramos, J. C.; Borges, D. L. G.; *J. Anal. At. Spectrom.* **2017**, *32*, 1893. [Crossref]
42. Guo, X. Q.; Tang, X. T.; He, M.; Chen, B. B.; Nan, K.; Zhang, Q. Y.; Hu, B.; *RSC Adv.* **2014**, *4*, 19960. [Crossref]
43. Depoi, F. S.; Bentlin, F. R. S.; Ferrao, M. F.; Pozebon, D.; *Anal. Methods* **2012**, *4*, 2809. [Crossref]
44. Karadas, C.; Kara, D.; *Water, Air, Soil Pollut.* **2014**, *225*, 1972. [Crossref]
45. Olajire, A. A.; *Chem. Eng. J. Adv.* **2020**, *4*, 100049. [Crossref]

Submitted: August 26, 2022

Published online: February 13, 2023

